Numerical analysis of crystal growth of an InAs-GaAs binary semiconductor under microgravity conditions

Toru Maekawa†, Yoshihiro Sugiki† and Satoshi Matsumoto††

† Toyo University

†† National Space Development Agency of Japan

We investigate the crystal growth process of an InAs-GaAs binary semiconductor by the Traveling Liquidus Zone (TLZ) method numerically and discuss the possibility of growing a bulk $In_{0.3}Ga_{0.7}As$ crystal. First, we review this new crystal growth technique and then explain a numerical model and calculation method of the growth of binary crystals. We focus on the effect of the solution zone width on the crystal growth process and the generation of supercooling in the solution in order to grow $In_{0.3}Ga_{0.7}As$. We find that a uniform $In_{0.3}Ga_{0.7}As$ can be grown by the TLZ method under 1 μg conditions by adjusting the solution zone width and the temperature gradient in the solution at appropriate values.

1. Introduction

Microgravity experiments of crystal growth have been carried out in recent years using drop towers, aircraft, rockets, space shuttles and satellites in order to reduce buoyancy convection and grow high quality crystals [1-8]. Now, the International Space Station is expected to come into operation in 2005 so that crystal growth experiments can be carried out under better conditions; that is, the long duration of low residual gravity conditions (~ 1 μg) is available.

Growing single crystals of uniform compositions of multi-component materials is very difficult compared to that of single-component materials since the shape and movement of the crystal–solution interfaces are determined by the concentration field in addition to the velocity and temperature fields. The interfacial temperature and concentration of the solute vary along the crystal–solution interfaces. We have studied the growth process of an InAs-GaAs binary crystal numerically and found that it is very difficult to grow a crystal of uniform compositions by the Bridgman method even under 1 μg conditions because of the high Schmidt number[9]. The concentration field is very sensitive to convection and is deformed easily by it due to the high Schmidt number. As a result, the crystal interfaces are deformed as the crystal growth proceeds. There is another important factor, which makes the growth of multi-component crystals difficult; that is, supercooling induced in the solution during the crystal growth process. Even under microgravity conditions, supercooling occurs in the solution due to the high Schmidt number [10].

In this report, we focus on the growth of a uniform binary single $In_{0.3}Ga_{0.7}As$ crystal under 1 μg conditions from a macroscopic point of view based on continuum thermofluid dynamics coupled with first-order phase transition. Having found that it is extremely difficult to grow an $In_{0.3}Ga_{0.7}As$ crystal by the Bridgman method [9], we employ a new crystal growth method named the Traveling Liquidus Zone (TLZ) method [12,13]. We review the TLZ method briefly in the next section. We explain a numerical model of crystal growth by the TLZ method in the third section. We show the result of the calculation and discuss the possibilities of growing a uniform single $In_{0.3}Ga_{0.7}As$ crystal by the TLZ method under 1 μg conditions in the forth section. In the final section, we summarize the results obtained in this study.

2. Traveling Liquidus Zone method

As we mentioned, the concentration field and the crystal–solution interfaces are seriously deformed and an $In_{0.3}Ga_{0.7}As$ crystal of uniform compositions

cannot be grown even under 1 μg conditions if $In_{0.3}Ga_{0.7}As$ crystals are grown by the Bridgman method due to the high Schmidt number. To improve this situation, Kinoshita *et al.* [12,13] proposed a new crystal growth method called the Traveling Liquidus Zone (TLZ) method. We summarize the basic idea of crystal growth by the TLZ method in the following (see also Fig.1): A solution is sandwiched between the seed and feed crystals. The difference between the TLZ method and the ordinary zone melting method is that the temperature and solute concentration gradients are kept constant in the solution in the growth direction during the growth process in the case of the TLZ method, whereas the initial concentration is usually constant in the seed and feed crystals and the solution in the case of the zone melting method. If there is no convection, the linear temperature and concentration distributions can be maintained in the solution, and crystal grows spontaneously in the case of the TLZ method. The linear temperature and concentration distributions in the solution coincide very closely with the liquidus curve on the phase diagram if the temperature difference between the two interfaces is small (see Fig.2 for the phase diagram of the InAs-GaAs binary system[6].). That is why this crystal growth method is called the Traveling Liquidus Zone method. However, supercooling always occurs in this case since the liquidus curve is, in fact, slightly convex (Fig.2). Therefore, reducing the degree of supercooling in the solution is very important in the case of the TLZ method. The temperatures and solute concentrations at the crystal–solution interfaces and the movement of the interfaces are determined by

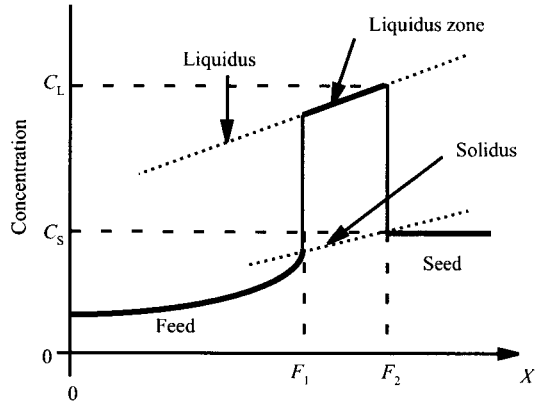

FIG.1 Traveling Liquidus Zone method. A linear concentration distribution is established in the solution and crystal grows naturally following Eq.(1). Therefore, if the heater is moved at the spontaneous crystal growth rate, a crystal of uniform compositions can be grown.

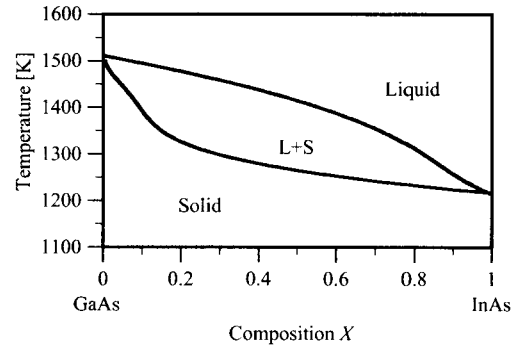

FIG.2 Pseudo-binary phase diagram of InAs–GaAs.

the heat and mass balance at the interfaces and the liquidus and solidus curves. The growth rate can be estimated as follows in the case of one-dimensional diffusion limited growth by the TLZ method [12,13]:

$$v = \frac{D}{(c_S - c_L)}\left(\frac{\partial c}{\partial T}\right)_{Liquidus}\left(\frac{\partial T}{\partial x}\right), \qquad (1)$$

where v is the growth rate of the seed crystal, D; the diffusion coefficient of the solute in the solvent, c_L; the saturation concentration of the solute at the solution side of the crystal–solution interface, c_S; the saturation concentration at the crystal side of the interface, $(\partial c/\partial T)_{Liquidus}$; the slope of the liquidus curve at the interfacial temperature, and $(\partial T/\partial x)$; the temperature gradient at the crystal–solution interface. The solute concentration decreases as crystal grows if the heater is not moved since the temperature at the seed crystal–solution interface rises with the movement of the interface. Therefore, if the heater is moved at the speed of the crystal growth rate v, the interfacial temperatures and concentrations can be kept constant at the crystal–solution interfaces during the crystal growth process. In other words, a crystal of uniform compositions can be grown. However, the temperature and concentration fields may be disturbed by convection even under 1 μg conditions. Therefore, we investigate the effect of convection on the crystal growth process by the TLZ method and estimate the optimal conditions for the production of uniform binary crystals in microgravity.

3. Numerical modeling and calculation method

In this section, we develop a numerical model of crystal growth by the TLZ method and introduce the governing equations of the growth of binary crystals. An outline of the numerical model of InAs–GaAs crystal growth is shown in Fig.3. The calculation area

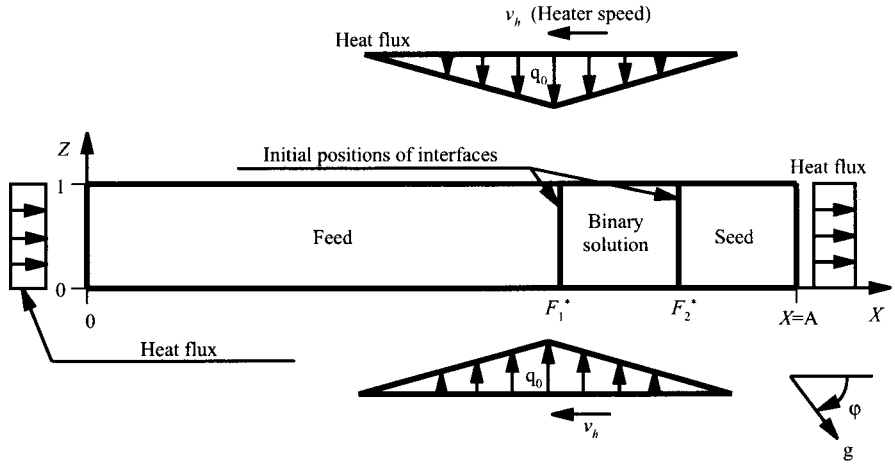

FIG.3 Outline of a crystal growth model of a binary InAs–GaAs semiconductor. A solution is sandwiched between seed and feed crystals. Heat flux is given externally from the top and bottom surfaces and the left-hand side wall. Heat is removed from the right-hand side wall. The velocity, temperature and concentration fields and the shape and movement of the interfaces are calculated numerically.

is divided into three regions: seed crystal, solution and feed crystal. The solution and the crystals are placed horizontally ($\varphi = 90°$) and the heat flux is applied externally as shown in Fig.3, which is based on the heater of the crystal growth experimental system of the Japanese experimental module (JEM) in the International Space Station. The top, bottom and left-hand side surfaces are heated and the right-hand side surface is cooled. The total amount of the heat input is equal to that of the heat output. The heaters move to the left so that the seed crystal grows in the $-x_1$ direction. The feed crystal–solution interface and the seed crystal–solution interface are, respectively, expressed by the following equations: $x_1 = F_1(x_2,t)$ and $x_1 = F_2(x_2,t)$. F_1 and F_2 are determined by the heat and mass balance at the interfaces and the liquidus and solidus curves on the phase diagram.

The coordinate x_i, time t, pressure p, velocity u_i and temperature T are nondimensionalized as follows:

$$X_i \equiv \frac{x_i}{L}, \quad \tau \equiv \frac{t}{L^2/\nu_L}, \quad U_i \equiv \frac{u_i}{\nu_L/L},$$

$$P \equiv \frac{p}{\rho_0 \nu_L^2/L^2}, \quad \theta \equiv \frac{T - T_f}{q_0 L/\lambda_L}, \tag{2}$$

where L, ν, ρ_0, q_0 and λ are, respectively, the depth of the solution layer, the kinematic viscosity, the density, the maximum value of the heat flux (see Fig.3) and the thermal conductivity. Subscripts L, S and f represent liquid, solid and the melting point of InAs. Note that the concentration of InAs is already nondimensionalized (see Fig.2). The nondimensional governing equations are given in the following:

A. Governing equations in solution

The Boussinesq approximation being employed for the density change, the continuity equation, the momentum equation, the energy equation and the transport equation of the solute are introduced as follows:

Continuity equation:

$$\frac{\partial U_i}{\partial X_i} = 0. \tag{3}$$

Momentum equation:

$$\frac{\partial U_i}{\partial \tau} + U_j \frac{\partial U_i}{\partial X_j} = -\frac{\partial P}{\partial X_i} + \frac{\partial^2 U_i}{\partial X_j \partial X_j} + \frac{Ra^T}{Pr}\theta_L k_i - \frac{Ra^C}{Sc} C_L k_i, \tag{4}$$

where the buoyancy forces caused by both the temperature and concentration differences are taken into account and k_i is the unit vector in the antigravitational direction. In the case of the InAs–GaAs system, the density increases with a decrease in temperature and with an increase in the concentration of InAs.

Energy equation:

$$\frac{\partial \theta_L}{\partial \tau} + U_j \frac{\partial \theta_L}{\partial X_j} = \frac{1}{Pr} \frac{\partial^2 \theta_L}{\partial X_j \partial X_j}. \tag{5}$$

Transport equation of concentration of InAs:

$$\frac{\partial C_L}{\partial \tau} + U_j \frac{\partial C_L}{\partial X_j} = \frac{1}{Sc} \frac{\partial^2 C_L}{\partial X_j \partial X_j}. \tag{6}$$

We do not take into account the Sorét effect in this study since it has very little effect on the crystal growth process in the case of the InAs-GaAs system[9]. Ra^T, Ra^C, Pr and Sc are, respectively, the Rayleigh number based on the temperature difference, the Rayleigh number based on the concentration difference, the Prandtl number and the Schmidt number:

$$Ra^T \equiv \frac{\beta g q_0 L^4}{\lambda_L \kappa_L \nu_L}, \quad Ra^C \equiv \frac{\gamma g \Delta C L^3}{D_L \nu_L},$$
$$Pr \equiv \frac{\nu_L}{\kappa_L}, \quad Sc \equiv \frac{\nu_L}{D_L}, \tag{7}$$

where β, g, κ_L, γ and D_L are, respectively, the temperature coefficient of volume expansion, the gravitational acceleration, the thermal diffusivity, the concentration coefficient of volume expansion and the diffusion coefficient of the solute.

B. Governing equations in crystal

The governing equations in the crystals are the heat conduction and diffusion equations.

Heat conduction equation:

$$\frac{\partial \theta_S}{\partial \tau} = \frac{K_{SL}}{Pr} \frac{\partial^2 \theta_S}{\partial X_j \partial X_j}. \tag{8}$$

Diffusion equation:

$$\frac{\partial C_S}{\partial \tau} = \frac{D_{SL}}{Sc} \frac{\partial^2 C_S}{\partial X_j \partial X_j}. \tag{9}$$

K_{SL} is the ratio of the thermal diffusivity of the crystal to that of the solution and D_{SL} is the ratio of the diffusion coefficient in the crystal to that in the solution:

$$K_{SL} \equiv \frac{\kappa_S}{\kappa_L}, \quad D_{SL} \equiv \frac{D_S}{D_L}. \tag{10}$$

C. Solution–Crystal interfaces

The temperature and concentration at the crystal–solution interfaces and the positions of the interfaces are determined by the heat and mass balance at the interfaces and the liquidus and solidus curves on the phase diagram. The phase diagram of the InAs-GaAs binary system is shown in Fig.2.

Heat balance at the interfaces:

$$\frac{\partial F_i^*}{\partial \tau} = \frac{Sf}{Pr} \left\{ \mp \left(\frac{\partial \theta_L}{\partial X_1} - \frac{\partial F_i^*}{\partial X_2} \frac{\partial \theta_L}{\partial X_2} \right) \right.$$
$$\left. \pm G_{SL} \left(\frac{\partial \theta_S}{\partial X_1} - \frac{\partial F_i^*}{\partial X_2} \frac{\partial \theta_S}{\partial X_2} \right) \right\}. \tag{11}$$

Mass balance at the interfaces:

$$(C_L - C_S) \frac{\partial F_i^*}{\partial \tau} = \frac{1}{Sc} \left\{ -\left(\frac{\partial C_L}{\partial X_1} - \frac{\partial F_i^*}{\partial X_2} \frac{\partial C_L}{\partial X_2} \right) \right.$$
$$\left. + D_{SL} \left(\frac{\partial C_S}{\partial X_1} - \frac{\partial F_i^*}{\partial X_2} \frac{\partial C_S}{\partial X_2} \right) \right\}. \tag{12}$$

Here, F_i^* is the interfacial position nondimensionalized by L, and i (= 1, 2) corresponds to interfaces 1 and 2 (see Fig.3). Double signs, $\mp$ and $\pm$, correspond to i = 1 and 2. G_{SL} is the ratio of the thermal conductivity of the crystal to that of the solution, and Sf is the Stefan number:

$$G_{SL} \equiv \frac{\lambda_S}{\lambda_L}, \quad Sf \equiv \frac{q_0 L}{\rho_0 L_{SL} \kappa_L}, \tag{13}$$

where L_{SL} is the latent heat per unit mass.

The temperature and concentration are not independent at the crystal–solution interfaces. The relations between the temperature and the concentration are given by the liquidus and solidus curves on the phase diagram. The temperature changes continuously at the interfaces; that is, $\theta_L = \theta_S$ at $X_1 = F_1^*$ and F_2^*, whereas concentration C_L is different from C_S at the interfaces. Since $\partial F_i^* / \partial \tau$ is common in Eqs.(11) and (12), the right-hand side of Eq.(11) is equal to the right-hand side of Eq.(12) divided by $(C_L - C_S)$. Therefore, the temperatures at the interfaces can be calculated. The interfacial temperatures having been determined, the concentrations at the interfaces are obtained via the liquidus and solidus curves and the positions of the interfaces F_i^* are calculated by Eq.(11). In this study, the relations between the concentrations and temperatures along the liquidus and solidus curves are approximated by polynomial functions of the fifth order. Here, we do not take into account the interfacial energy of the crystal–solution interfaces, that is, the Gibbs-Thompson effect[9,14], which has a crucial effect when the radius of the interfacial curvature is very small.

D. Numerical method and procedure

Since the crystal–solution interfaces move and the interfacial shapes change during the crystal growth process, we employ the boundary fit method to solve the governing equations efficiently[16].

Let us summarize the calculation procedure:

(1) The feed crystal–solution and seed crystal–solution interfaces are planar initially. The initial concentration of InAs in the seed crystal

Table 1 Physical properties, system dimensions and growth conditions

Kinematic viscosity	ν_L	[$m^2 s^{-1}$]	1.5×10^{-7}
Density	ρ_0	[$kg\ m^{-3}$]	5.9×10^4
Thermal conductivity of solution	λ_L	[$W\ m^{-1} K^{-1}$]	3.0
Thermal conductivity of crystal	λ_S	[$W\ m^{-1} K^{-1}$]	1.2
Temperature coefficient of volume expansion	β	[K^{-1}]	9.34×10^{-5}
Concentration coefficient of volume expansion	γ	[–]	1.4×10^{-1}
Thermal diffusivity of solution	κ_L	[$m^2 s^{-1}$]	1.1×10^{-5}
Thermal diffusivity of crystal	κ_S	[$m^2 s^{-1}$]	3.0×10^{-6}
Diffusion coefficient of In in solution	D_L	[$m^2 s^{-1}$]	1.5×10^{-8}
Diffusion coefficient of In in crystal	D_S	[$m^2 s^{-1}$]	1.0×10^{-11}
Latent heat	L_{SL}	[$J\ kg^{-1}$]	5.0×10^5
Depth of solution and crystal	L	[mm]	10, 20
Width of solution and crystal	W	[mm]	120
Heater speed	v_h	[$mm\ h^{-1}$]	0.2, 0.4

is 0.3, which is our target value, and that in the feed crystal is set at a constant value, which depends on the initial temperature gradient in the solution and the initial solution zone width. The concentrations at the solution sides of the interfaces are determined by the liquidus curve on the phase diagram. The concentration is linearly distributed in the solution and linear temperature distributions are given along the solution and crystals initially. Note that the temperatures at the interfaces are set at the equilibrium values corresponding to the interfacial concentrations.

(2) We start heating and cooling the system externally as shown in Fig.3. Note that the Rayleigh number is defined using q_0, which is the maximum value of the heat flux from the heater (see Fig.3).

(3) We solve the governing equations (3)-(6), (8) and (9) to obtain the velocity, temperature and concentration fields in the solution, and seed and feed crystals.

(4) The interfacial temperature and concentration are determined by the heat and mass balance equations and the liquidus and solidus curves on the phase diagram (see section **3.C**).

(5) The interfacial temperature having been determined, the time derivatives of the crystal–solution interfaces are calculated by Eq.(11) and therefore the new positions of the interfaces are obtained. Using the new interfacial temperatures and concentrations and the new interfacial positions, procedures (3)-(5) are repeated.

The nondimensional parameters are estimated based on the physical properties of InAs and GaAs [16,17]. The residual gravity is 1 μg (= 10^{-6} g). The depth of the solution and crystals is 10 mm; the aspect ratio of the system, A, is set at 12; and the initial position of the seed crystal–solution interface, F_2^*, is set at X_1 = 10. The initial position of the feed crystal–solution interface, F_1^*, is changed depending on the initial width of the solution zone. The maximum heat flux q_0 is 1.0 kW/m^2. The initial temperature gradient in the solution is 10 or 20 K/cm. The heater speed is set at 0.2 and 0.4 mm/h, which are the growth rates corresponding to the temperature gradients in the solution; 10 and 20 K/cm, in the case of the one-dimensional diffusion limited crystal growth (see Eq.(1)). The physical properties, system dimensions and growth conditions are summarized in Table 1.

The calculation space is divided by 123 × 31, 163 × 41 and 203 × 51 finite difference grids and the maximum differences in the stream function, temperature, concentration and positions of the interfaces caused by the differences in the number of the grid points were within 2 %. The results shown in the following section are based on the calculations using 163 × 41 grid points.

4. Results and discussion

We investigate the effect of the initial zone width of the solution on the crystal growth process. The time variations of the maximum velocity of convection induced in the solution under 1 μg conditions are

shown in Fig.4(a), where the depth of the solution is 10 mm and the zone width is changed from 10 to 60 mm, and the maximum velocity under 1 g conditions is shown in Fig.4(b) for comparison, where the depth and width of the solution are 10 mm. The maximum velocity induced in the solution, the depth and width of which are, respectively, 20 mm and 40 mm, under 1 μg conditions is also shown in Fig.4(c). In all of the above cases (Figs.4(a)-(c)), the initial temperature gradient in the solution is 10 K/cm. As the solution zone width increases, the maximum velocity increases (Fig.4(a)). The maximum velocity under 1 μg conditions is less than 1 μm/s when the depth of the solution is 10 mm (Fig.4(a)), whereas the order of the maximum velocity under 1 g conditions is several mm/s (Fig.4(b)). Velocity in the solution is reduced remarkably under 1 μg conditions. When crystals are grown in the horizontal direction under terrestrial gravitational conditions, strong buoyancy convection is driven in the solution even if the width of the solution is as narrow as 10 mm. If the depth of the solution is increased to 20 mm under 1 μg conditions, the maximum velocity increases up to approximately 3 μm/s (Fig.4(c)). The larger the crystal size is, the stronger becomes buoyancy convection.

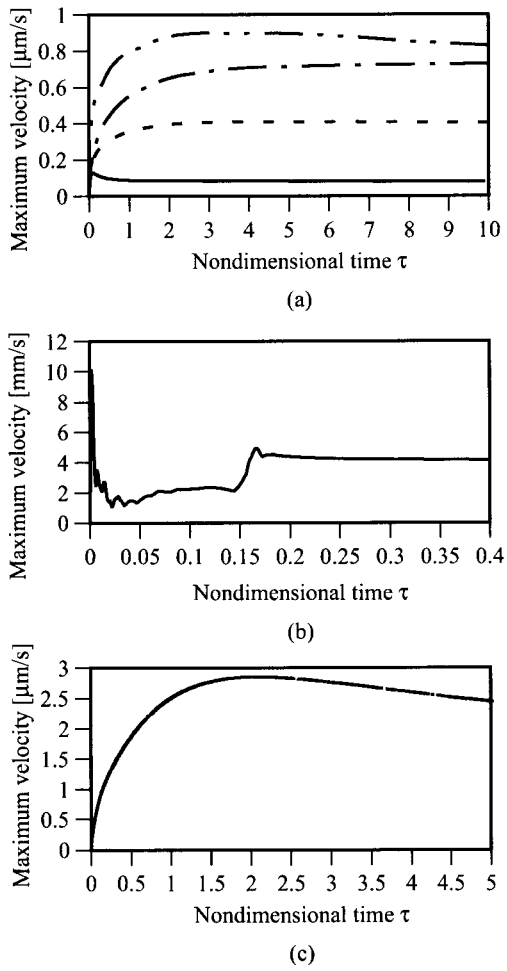

FIG.4 Time variations of maximum velocity in the solution. The temperature gradient in the solution is 10 K/cm. (a) The depth of the solution is 10 mm. The residual gravity is 1 μg. ——— : the solution zone width is 10 mm; -------- : 20 mm; – – – – – : 40 mm; – – – – – – : 60 mm. (b) The depth of the solution is 10 mm. A terrestrial gravitational acceleration of 1 g is applied. (c) The depth of the solution is 20 mm and the solution zone width is 40 mm. The residual gravity is 1 μg.

Snapshots of the streamlines, isotherms, isoconcentration lines and the shapes of the interfaces are shown in Fig.5. The initial temperature gradient in the solution is 10 K/cm. The concentration and temperature fields and the shape of the seed crystal –solution interface are hardly deformed and the concentration distribution in the solution in the growth direction is almost linear, which is very suitable for crystal growth by the TLZ method, when the depth and width of the solution is 10 mm (Fig.5(a)), while the concentration field becomes slightly asymmetric and the concentration is not linearly distributed in the solution any more when the width of the solution is 40 mm, in which case the concentration of the solute in the grown crystal cannot be constant (Fig.5(b)). If crystal is grown under 1 g conditions, on the other hand, the temperature and concentration fields are seriously disturbed by buoyancy convection and therefore the initial concentration gradient cannot be maintained at all (Fig.5(c)). It is quite remarkable that even under 1 μg conditions, when the depth is increased to 20 mm, the concentration field is deformed and the initial concentration gradient cannot be maintained in the solution (see Fig.5(d)).

The dependence of the steady-state crystal growth rate at the center of the seed crystal–solution interface on the initial solution zone width is shown in Fig.6, where the depth of the solution is 10 mm, the initial temperature gradient in the solution is 10 K/cm and the growth rate under 0 g conditions is also shown for comparison. The growth rate increases with the zone width and the growth rate at the center under 1 μg conditions is almost the same as that under 0 g conditions, although the shape of the interface is not completely symmetric under 1 μg conditions (see also Fig.7). Due to the input heat flux distributions and the heat release from the right-hand side wall, the temperature and concentration are not completely

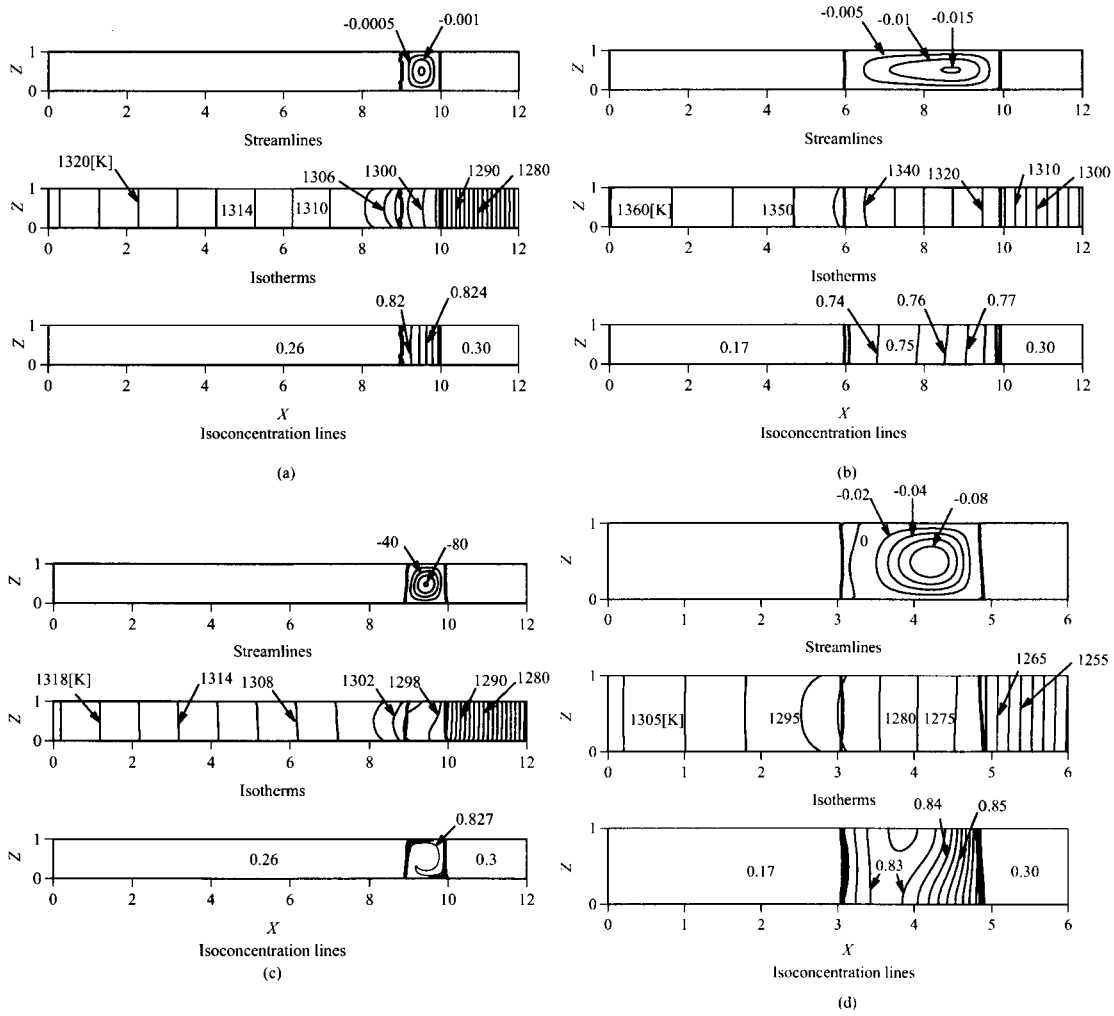

FIG.5 Streamlines, isotherms, isoconcentration lines and shapes of the crystal–solution interfaces. The initial temperature gradient in the solution is 10 K/cm. (a) The depth and initial zone width of the solution are 10 mm. 1 μg is applied. Ra^T = 1.85× 10^{-3}; Ra^C = 6.10× 10^2; τ = 10. (b) The depth and initial zone width of the solution are, respectively, 10 mm and 40 mm. 1 μg is applied. Ra^T = 1.85× 10^{-3}; Ra^C = 6.10× 10^2; τ = 10. (c) The depth and initial zone width of the solution are 10 mm. 1 g is applied. Ra^T = 1.85× 10^3; Ra^C = 6.10× 10^8; τ = 5. (d) The depth and initial zone width of the solution are, respectively, 20 mm and 40 mm. 1 μg is applied. Ra^T = 2.96× 10^{-2}; Ra^C = 4.88× 10^3; τ = 5.

linearly distributed in the solution and the temperature and concentration gradients at the solution side of the seed crystal–solution interface become greater as the solution becomes wider, which accounts for the increase in the crystal growth rate. If the temperature and concentration gradients were maintained at the initial values in the solution, the crystal growth rate would be constant irrespective of the zone width (see Eq.(1)). Note that the crystal growth rate under 1 g conditions is increased to 0.8 mm/h and the rate under 1 μg conditions when the depth of the solution is 20 mm is 0.56 mm/h. In both cases, the crystal growth rate is much higher than that in the one-dimensional diffusion limited case.

The time variations of the seed crystal–solution interface are shown in Fig.7. The crystal growth rate increases and the growth rate at the upper part of the crystal becomes higher than that at the lower part as the zone width increases since buoyancy convection is intensified and the amount of the solute transported towards the crystal increases with the increase in the zone width (Figs.7(a)-(c)). In the case of crystal growth under 1 g conditions, the shape of the crystal–solution interface is seriously deformed (Fig.7(d)). Even when crystal is grown under 1 μg conditions, the crystal–solution interface is deformed if the depth of the solution is 20 mm (Fig.7(e)).

The distributions of the solute concentration

along the center of the grown crystals under 1 μg conditions are shown in Fig.8, where the depth of the solution is 10 mm and the initial temperature gradient in the solution is 10 K/cm. The concentration decreases as crystal grows when the initial solution zone width is 20 mm (Fig.8(a)), while it increases when the zone width is 5 mm (Fig.8(c). Note that melt-back occurs in the early stage.). In the present case, the solution zone width should be 10 mm for the growth of crystals of uniform compositions (Fig.8(b)). The distribution of the InAs concentration in the grown crystal is altered dramatically depending on the initial solution zone width. However, even when the initial solution zone width is 10 mm, the concentration in the grown crystal decreases as crystal grows if the temperature gradient in the solution is 20 K/cm (see Fig.9).

Finally, we check the effect of the initial solution zone width on the degree of supercooling induced in the solution. The degree of supercooling is defined as follows:

$$S \equiv \frac{C_L - C_{L,sat}}{C_{L,sat}}, \qquad (14)$$

where C_L is the local concentration in the solution and $C_{L,sat}$ is the saturation concentration corresponding to the local temperature (see the liquidus curve on the phase diagram (Fig.2).). The area where S is negative is supercooled. The dependence of the maximum value of the degree of supercooling, $|S|_{max}$, on the initial solution zone width is shown in Fig.10, where the depth of the solution is 10 mm and the initial temperature gradient in the solution is 10 K/cm. In the case of the TLZ method, supercooling is induced in the solution in general (see also Fig.2), but it can be reduced by reducing the solution zone width.

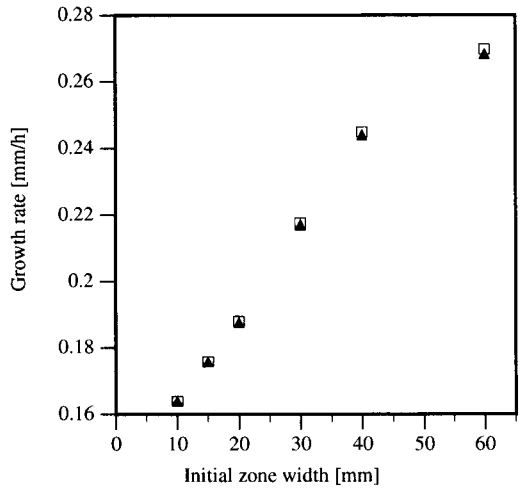

FIG.6 Steady-state crystal growth rate at the center of the seed crystal–solution interface. The depth of the solution is 10 mm and the initial temperature gradient in the solution is 10 K/cm.

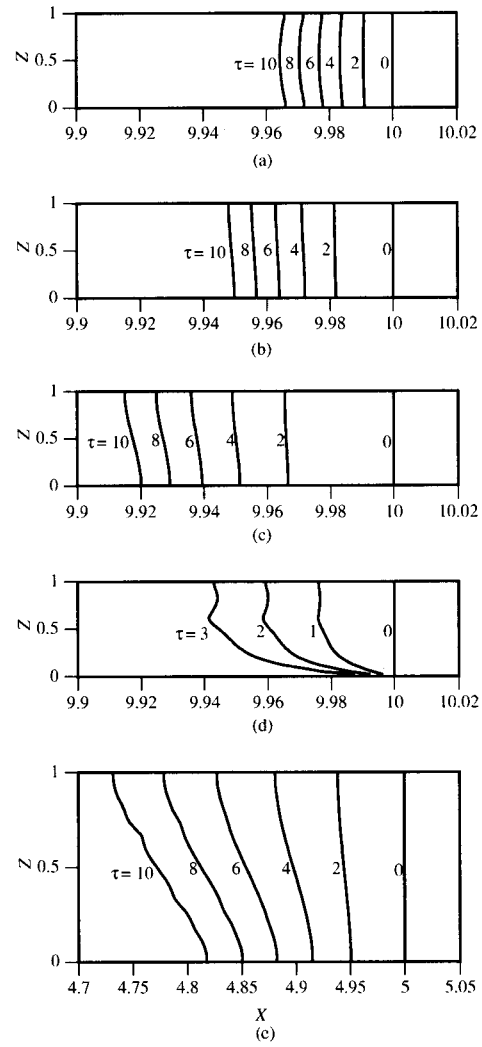

FIG.7 Time variations of the seed crystal–solution interface. The initial temperature gradient in the solution is 10 K/cm. (a) The depth and initial zone width of the solution are 10 mm. 1 μg is applied. (b) The depth and initial zone width are 10 mm and 20 mm. 1 μg is applied. (c) The depth and initial zone width are 10 mm and 40 mm. 1 μg is applied. (d) The depth and initial zone width are 10 mm. 1 g is applied. (e) The depth and initial zone width are 20 mm and 40 mm. 1 μg is applied.

In summary, we investigated the crystal growth process of an InAs–GaAs semiconductor numerically and found that it is quite possible to grow a high quality $In_{0.3}Ga_{0.7}As$ crystal by the TLZ method by setting the initial solution zone width and the temperature gradient in the solution at appropriate

values so that buoyancy convection and the degree of supercooling are reduced and the solute concentration becomes constant in the grown crystal. We set the initial temperature gradient in the solution at 10 K/cm in this study. If the temperature gradient is higher than 10 K/cm, buoyancy convection becomes stronger and the degree of supercooling becomes higher. We should reduce the temperature gradient in the solution so that both buoyancy convection and supercooling are reduced, but if the temperature gradient is lower than 10 K/cm, the heater speed should be very slow and the control of the interfacial temperatures becomes very difficult. We, therefore, propose the following conditions for the growth of an $In_{0.3}Ga_{0.7}As$ of 10 mm in size from a practical point of view: the temperature gradient in the solution, 10 K/cm; the solution zone width, 10 mm; the heater speed, 0.2 mm/h. However, as we have shown, it is still difficult to grow larger binary crystals of uniform compositions even under 1 μg conditions. We need other innovative ideas to overcome this problem.

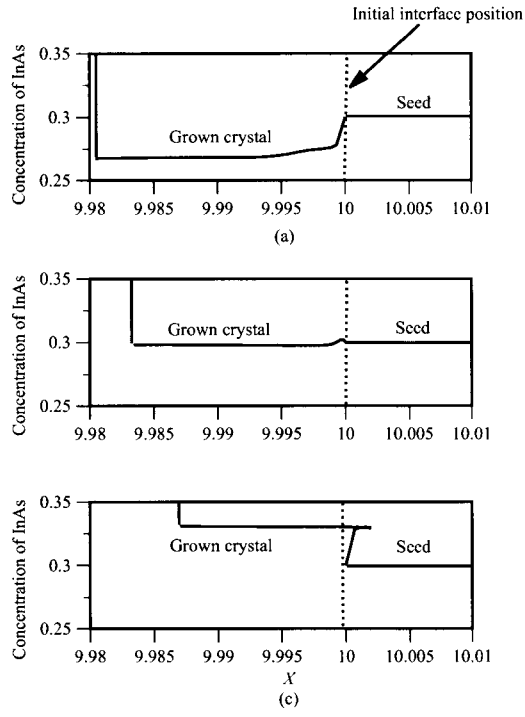

FIG.8 Distributions of the solute concentration along the center of the grown crystal. The depth of the solution is 10 mm and the initial temperature gradient in the solution is 10 K/cm. 1 μg is applied. (a) The initial zone width is 20 mm; $\tau = 3$; (b) 10 mm; $\tau = 7$; (c) 5 mm; $\tau = 7$.

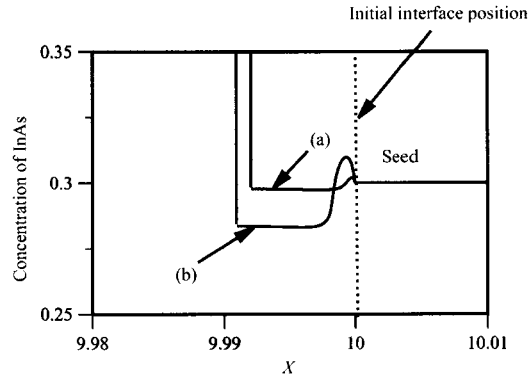

FIG.9 Distributions of the solute concentration along the center of the grown crystal. The depth and the zone width of the solution are 10 mm. 1 μg is applied. $\tau = 3$. (a) The initial temperature gradient in the solution is 10 K/cm; (b) 20 K/cm.

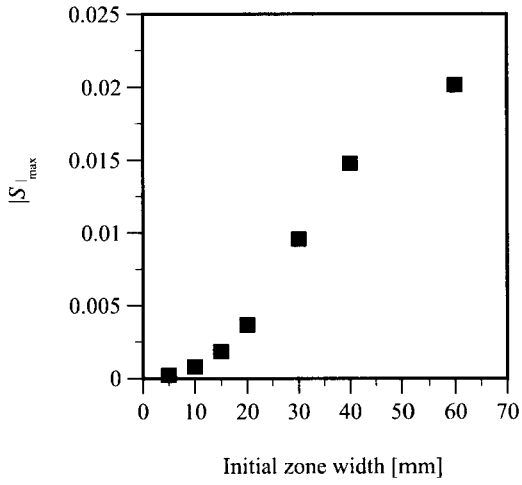

FIG.10 Dependence of the degree of supercooling on the initial solution zone width. The depth of the solution is 10 mm. The initial temperature gradient in the solution is 10 K/cm. 1 μg is applied.

5. Conclusions

We investigated the possibility of growing an $In_{0.3}Ga_{0.7}As$ crystal by the Traveling Liquidus Zone (TLZ) method under 1 μg conditions numerically. We developed a numerical model of growth of a binary InAs–GaAs crystal and a numerical method based on the finite difference and boundary fit methods. We have obtained the following results through the numerical analysis: (a) Convection is reduced by reducing the solution depth and the solution zone width under microgravity conditions. The maximum velocity of convection induced in the

solution is less than 1 μm/s when the solution depth is 10 mm under 1 μg conditions. (b) The temperature and concentration fields and the shape of the crystal interfaces are not seriously deformed when the depth and width of the solution are 10 mm. However, as the solution zone width increases, the shape of the crystal interface becomes asymmetric. (c) The crystal growth rate under 1 μg conditions is more or less the same as that under 0 g conditions. (d) The distribution of the solute concentration in the grown crystal is changed by the initial solution zone width and the initial temperature gradient in the solution. (e) Supercooling generated in the solution is reduced by reducing the solution zone width.

In summary, a uniform $In_{0.3}Ga_{0.7}As$ crystal of 10 mm in size can be grown by the TLZ method under 1 μg conditions by setting the initial solution zone width and the temperature gradient in the solution at 10 mm and 10 K/cm, respectively, in which case buoyancy convection and supercooling are greatly reduced and the concentration of In in the grown crystal becomes constant.

References

1 K. Kinoshita and K. Sugii, J. Crystal Growth **67**, 375 (1984).
2 K. Kinoshita and K. Sugii, J. Crystal Growth **71**, 283 (1985).
3 H.U. Walter (ed), Fluid Sciences and Materials Science in Space (Springer, Tokyo, 1987).
4 K. Nakajima, T. Kusunoki and C. Takenaka, J. Crystal Growth **113**, 485 (1991).
5 A. Baldus and K.W. Benz, J. Crystal Growth **130**, 37 (1993).
6 P. Höschl, R. Grill, J. Svoboda, P. Hlídek, P. Moravec, J. Franc and E. Belas, J. Crystal Growth **138**, 956 (1994).
7 T. Kusunoki, C. Takenaka and K. Nakajima, J. Crystal Growth **112**, 33 (1991).
8 P. Höschl, R. Grill, J. Svoboda, P. Hlídek, P. Moravec, J. Franc and E. Belas, J. Crystal Growth **138**, 956 (1994).
9 Y. Hiraoka, K. Ikegami, T. Maekawa, S. Matsumoto, S. Yoda and K. Kinoshita, J. Phys. D: Appl. Phys. **33**, 2508 (2000).
10 S. Matsumoto and T. Maekawa, Adv. Space Res. **24**, 1215 (1999).
11 P. Bhattacharya, Properties of Lattice-Matched and Strained Indium Gallium Arsenide (INSPEC, London, 1993).
12 K. Kinoshita, K. Kato,T. Tsuru, Y. Muramatsu and S. Yoda, J. Crystal Growth **225**, 59 (2001).
13 K. Kinoshita, Y. Hanaue, H. Nakamura, S. Yoda, M. Iwai, T. Tsuru and Y. Muramatsu, J. Crystal Growth **237-239**, 1859 (2002).
14 S.R. Coriell and G.B. McFadden, Morphological Stability Handbook of Crystal Growth vol.1b, ch.12, pp.785-857 (North-Holland, Amsterdam, 1993).
15 J.F. Thompson, Z.U.A. Warsi and C.W. Mastin, Numerical Grid Generation: Foundations and Applications (Elsevier, New York, 1985).
16 V.M. Glazov, S.N. Chizhevskaya and N.N. Glagoleva, Liquid Semiconductors (Plenum New York, 1969).
17 K.H. Hellwege, Landolt-Börnstein: Numerical Data and Functional Relationships in Science and Technology vol.17 (Springer, Berlin, 1982).